A novel immunological approach establishes that the auxin-binding protein, Nt-abp1, is a element involved in auxin signaling at the plasma membrane

Nathalie Leblanc, Karine David, Jeanne Grosclaude, Jean-Marc Pradier,
Hélène Barbier-Brygoo, Suzanne Labiau, Catherine Perrot-Rechenmann

▶ **To cite this version:**

HAL Id: hal-02685296
https://hal.inrae.fr/hal-02685296

Submitted on 1 Jun 2020

A Novel Immunological Approach Establishes That the Auxin-binding Protein, Nt-abp1, Is an Element Involved in Auxin Signaling at the Plasma Membrane*

Nathalie Leblanc‡§¶, Karine David‡¶, Jeanne Grosclaude‖, Jean-Marc Pradier‡,
Hélène Barbier-Brygoo‡‡, Suzanne Labiau‖, and Catherine Perrot-Rechenmann‡§§**

*From the ‡Group of Auxin Perception and Transport, Institut des Sciences Végétales, CNRS, 91198 Gif sur Yvette,
Cedex, France, ‖ Laboratoire de Virologie et Immunologie Moléculaires, Institut National de la Recherche Agronomique,
78352 Jouy en Josas, France, and the ‡‡Group of Transmembrane Transporters, Institut des Sciences Végétales,
CNRS, 91198 Gif sur Yvette, Cedex, France*

Interactions of a collection of monoclonal antibodies (mAbs) to the recombinant *Nicotiana tabacum* auxin-binding protein 1 (Nt-abp1) were extensively characterized using surface plasmon resonance. Dynamic interaction studies using combinations of Nt-abp1, synthetic peptides corresponding to conserved sequences within auxin-binding proteins, and the mAbs have shown that a number of the mAbs recognized discontinuous epitopes revealing the junction of distinct domains in the folded protein. In particular, the two putative auxin binding domains and the C terminus of the protein were shown to interact with each other in the folded protein. Using the auxin-induced electrical response of tobacco protoplasts as a functional assay, all the mAbs exhibited either auxin antagonist or hormonomimetic properties. These effects, measured for the first time in homologous conditions, confirm that Nt-abp1 is present at the plasma membrane and is involved in the activation of the auxin-dependent electrical response of tobacco protoplasts. Based on our surface plasmon resonance data, we propose that the key event leading to the activation of this auxin electrical response consists of a conformational change in Nt-abp1.

The plant hormone auxin controls alone or in concert with other plant hormones a wide range of plant growth and developmental processes including cell division, cell elongation, lateral and adventitious root formation, tropisms, and cell differentiation (1). The molecular mechanisms of auxin action are still poorly understood, although recent advances resulting from molecular studies of auxin-regulated genes and genetic approaches have contributed to the identification of transcription factors, some with defined genetic function, and to the demonstration that the regulated protein degradation by the

ubiquitin-proteosome pathway plays a key role in auxin action (2–5).

Within the last 10 years, biochemical approaches have been developed with the objective of identifying auxin receptors. A number of soluble and membrane-associated auxin-binding proteins have been described. However, in most cases their functional role in signaling, transport, or metabolism of auxin remains unclear (6, 7). Even the function of the most studied auxin-binding protein (ABP1)[1] remains elusive. Maize ABP1 (Zm-abp1), a soluble protein initially isolated from maize coleoptiles (8, 9), was rapidly designated as a possible auxin receptor. This hypothesis depended mainly on electrophysiological studies (10–14). Electrophysiological responses to auxin reflect the modulation of membrane ion transport as a rapid response (less than 1 min) to auxin action at the outer face of the plasma membrane (15). The involvement of ABP1 or an immunologically related protein was mainly suggested by a series of electrophysiological experiments with the maize protein (10), polyclonal antibodies to Zm-abp1 (10, 11), or C-terminal Zm-abp1-derived synthetic peptides using either *Vicia faba* guard cells (14) or tobacco protoplasts (16) as plant materials. Thus, these data have been obtained by using heterologous tools for distinct electrical measurements. Most of the polyclonal antibodies to Zm-abp1 are mapped close to its *N*-glycosylation site interacting with a restricted region of the protein (17), weakening the reported data, and compromising their use to further investigate the involvement of ABP1 in auxin signaling. At the moment, the involvement of ABP1 as an auxin receptor is based on the accumulation of weak evidence and remains open to question, as reflected in a provocative paper by Hertel (18). Recently, interest in ABP1 was brought up to date by work in which transgenic plants overexpressing ABP1 were shown to exhibit an increased capacity for auxin-mediated cell expansion (19), establishing a relationship between the expression of ABP1 and this auxin growth response. In addition, we have recently shown that the tobacco protein alone induces the activation of the electrical membrane response of tobacco mesophyll protoplasts (20) reinforcing the correlation between ABP1, auxin, and the early electrical response.

To further characterize ABP1 and investigate its possible role in auxin signaling, we have assembled specific tools and functional responses for a single plant material. Modification of

[1] The abbreviations used are: ABP1, auxin-binding protein 1; NAA, 1-naphthaleneacetic acid; mAb, monoclonal antibody; Nt-abp1, *Nicotiana tabacum* auxin-binding protein 1; RU, resonance unit; Zm-abp1, *Zea maïs* auxin-binding protein 1; ELISA, enzyme-linked immunosorbent assay.

the transmembrane electrical potential of tobacco protoplasts in response to auxin was one of the earliest responses related to the perception of auxin at the plasma membrane to be reported (15). Following the isolation of the tobacco ABP1 cDNA (21), we have developed a panel of monoclonal antibodies (mAbs) to the recombinant Nt-abp1 allowing experiments to be performed in homologous conditions. The interaction between these mAbs and Nt-abp1 has been extensively characterized using a bio-sensor-based analytical system to provide real-time measurements. This method has allowed for the first time detailed analysis of the three-dimensional configuration of the protein, and we report a unique picture of the folding of Nt-abp1. The present work clarifies the involvement of Nt-abp1 in an early auxin response. Our results are discussed in relation to the idea that different conformational states of Nt-abp1 mediate transduction of the auxin signal at the plasma membrane.

EXPERIMENTAL PROCEDURES

Materials—The recombinant tobacco protein, Nt-abp1, was produced in *Escherichia coli* and purified as described by Leblanc *et al.* (21). Zm-abp1 was extracted and purified from microsomal fractions of maize coleoptiles as described previously (22). Four synthetic peptides corresponding to Nt-abp1 domains have been used. Their sequences correspond to particular domains of ABP1 proteins: RTPIHRHSCEEIFIV-LKG, named pep A, corresponds to the conserved box A suspected to be involved in the binding of auxin (23); EHEDLQVLDVISRPP, named pep B, corresponds to the highly conserved box B; VFMYDDWSMPH-TAAKLKFP, named pep C, corresponds to the peptide 11 found by Brown and Jones (24) to be labeled by azidoindole-3-acetic acid; and WDEDCYQTTSWKDEL, named C-term, corresponds to the C-terminal domain of Nt-abp1 (20). Peptides A, B, and C were provided by A. Jones (University of North Carolina) via the Micro Protein Chemistry Facility, and pep C-term was synthesized and purified in the laboratory of J. Igolen (Institut Pasteur, Paris).

Antibody Production—A BALB/c mouse was injected intraperitoneally with 24 μg of purified *E. coli* Nt-abp1 emulsified in Freund's complete adjuvant. Two other boosts of antigen were given 2 and 3 months later 3 days before fusion. Fusion of splenocytes with SP$_2$O-Ag14 myeloma cells was carried out with 1 ml of 45% polyethylene glycol following the procedure described by Nowinsky *et al.* (25). After initial screening of hybridomas by enzyme-linked immunosorbent assay (ELISA), selected hybridomas were subcloned to ensure monoclonality. Strong positive clones were propagated in mice to produce ascitic fluids. Monoclonal isotypes were determined using the Serotec kit (Argene).

Immunoassays—The initial screening of culture supernatants was done by ELISA. Microwell plates (Falcon) were coated with 100 μl of purified *E. coli* Nt-abp1 (0.5 μg/ml) in phosphate-buffered saline (10 mM phosphate buffer, pH 7.4, 120 mM NaCl, 2.7 mM KCl) containing 4 μg/ml fat-free milk proteins for 90 min at 37 °C and then incubated overnight at 4 °C. Control wells were coated in the same conditions with fat-free milk proteins (4 μg/ml) or proteins extracted from nonrecombinant *E. coli* cells (4 μg/ml). Incubation with the supernatants (dilution 1/2) was followed by incubation with an anti-mouse IgG antibody conjugated to alkaline phosphatase. Enzymatic activity was revealed using *p*-nitrophenyl phosphate in 1 mM diethanolamine, pH 9.8, 10 mM MgCl$_2$.

For Western blot analysis, proteins were separated by SDS-polyacrylamide gel electrophoresis analysis on 12.5% (w/v) polyacrylamide gels and transferred electrophoretically to nitrocellulose membranes (HybondC, 0.45 μm, Amersham Pharmacia Biotech). After blocking with 5% fat-free milk, membranes were incubated with monoclonal antibodies to Nt-abp1 (ascitic fluids diluted at 1:1000) for 1 h in Tris-buffered saline Tween (250 mM NaCl, 50 mM Tris-HCl, pH 7.6, 0.1% Tween 20). After washing in Tris-buffered saline Tween, the bound antibodies were detected by goat anti-mouse IgG-alkaline phosphatase conjugate (Biosys, diluted at 1:1000). Membranes were then transferred in 50 mM Tris acetate, pH 9.7, 10 mM magnesium acetate, and the enzymatic activity was revealed using 5-bromo-4-chloro-3-indoyl phosphate/nitro blue tetrazolium chloride (Bio-Rad) as substrates.

BIAcore Analysis: Coupling of Nt-abp1 and the Synthetic Peptides to CM-Dextran—The analytical system, BIAcore (Amersham Pharmacia Biotech), based on surface plasmon resonance (26, 27), was used to extensively characterize the interaction of mAbs with Nt-abp1 whole protein or domains. Purified *E. coli*-produced Nt-abp1 was biotinylated using photoactivable biotin (CLONTECH) as described by Lacey and Grant (28), and about 10,000 RU avidin D (Vector) were first covalently

immobilized by aminolink to CM-dextran under standard conditions (26). Biotinylated Nt-abp1 was injected at concentrations ranging from 40 to 100 μg/ml under a flow of 10 μl/min for 8 min. In these conditions, 500–2000 RU were immobilized on the linked avidin. The different peptides were immobilized by aminolink on a hyperactivated CM-dextran matrix. Hyperactivation was performed by injection of 50 mM *N*-ethyl-*N'*-(3-diethylaminopropyl)carbodiimide/*N*-hydroxysuccinimide in HBS (25 mM Hepes buffer, pH 7.4, 150 mM NaCl, and 0.05% P20) for 20 min at flow 2 μl/min. The peptides of acidic pI were injected at a concentration of 500 μg/ml in 10 mM sodium formate buffer at pH 3.5, and the peptides of alkaline pI were injected at the same concentration in 5 mM maleate buffer, pH 6.0. Unreacted sites were blocked with a 25-min injection of 1 M ethylenediamine hydrochloride, pH 7.8, at 2 μl/min.

mAb Interactions—The reactivity of each mAb was checked by injection of 30 μl of diluted ascitic fluids or hybridoma supernatants at a final concentration of about 0.3 μM immunoglobulin. Standard mAb binding experiments were performed under a flow of 5 μl/min in HBS. After each experiment, the antibodies were removed by a short pulse of 8 μl of 100 mM HCl. Under these conditions, Nt-abp1 antigenicity was well conserved for 40–50 runs. Interaction of mAbs with Nt-abp1 has also been investigated at pH 5.7 in 15 mM maleate buffer, 150 mM NaCl, and 0.05% P20.

Interference Map—Pairwise epitope mapping was conducted under two distinct conditions. Competition assays were first performed on the immobilized biotinylated Nt-abp1. Three 40-μl sequential injections of the first mAb, ensuring exhaustive binding to the corresponding epitope, were followed by one injection of a second mAb. Each mAb was successively used as a first or second mAb. In a distinct set of experiments, a sandwich procedure was performed as follows: on immobilized rabbit anti-mouse antibody the first mAb to Nt-abp1 was captured; then the purified Nt-abp1 was injected followed by one injection of a second mAb.

Competition Binding Assays—Monoclonal antibodies were incubated in the presence of a 30-fold excess of peptide (mole of mAb/mole of peptide) before injection on the biosensors consisting of immobilized Nt-abp1 or of the individual synthetic peptides. The capture of the mAbs in the presence of the synthetic peptides was compared with their capture on the same biosensor in the absence of the peptide competitors.

Measurement of the Electrical Response of Tobacco Protoplasts—The effects of mAbs to *E. coli*-produced Nt-abp1 were tested on mesophyll protoplasts from young tobacco leaves (*Nicotiana tabacum* cv. Xanthi, wild-type clone XHFD8) isolated as described previously (29). For each experiment, aliquots (100 μl) of the protoplast suspension (5×10^4 protoplasts/ml) were incubated with different concentrations of IgGs for 5 min at room temperature. The membrane potential E_m was measured as described previously (30) directly or after the addition of NAA 3×10^{-6} M in the external medium. Dose-response curves were established by plotting ΔE_m values as a function of antibody concentration. For these experiments, mAb 12 IgG1 was purified using recombinant protein A/G affinity chromatography (Pierce), and mAb 37 IgM was precipitated with ammonium sulfate from culture supernatants. In all experiments, controls were performed with nonspecific IgGs or IgMs prepared in the same conditions.

RESULTS

Production and Characterization of Monoclonal Antibodies—Recombinant Nt-abp1, purified from *E. coli*, was used for mouse immunization to raise monoclonal antibodies. About 70 culture supernatants of hybridomas derived from one fusion were tested by ELISA allowing the selection of 9 positive clones. Antibody isotyping revealed that 4 of these mAbs were IgMs (mAbs 15, 37, 43, and 49), whereas the others corresponded to IgG1 type (mAbs 12, 17, 28, and 34) or IgG3 type (mAb 50). In further experiments, we concentrated on the characterization of the IgG1-type and two IgM-type (mAbs 15 and 37) antibodies.

The immunoblot presented in Fig. 1 shows that mAbs 12, 17, 28, and 34 recognize the recombinant protein Nt-abp1 purified from bacterial extracts (*lane 1*) as well as the maize protein purified from maize coleoptiles (*lane 2*). mAbs 12 and 28 recognize the maize protein as well as the tobacco protein. The ability of mAb 17 and mAb 34 to detect Zm-abp1 appears to be lower than for Nt-abp1, which suggests that the epitopes recognized by these two mAbs are not strictly conserved in Zm-
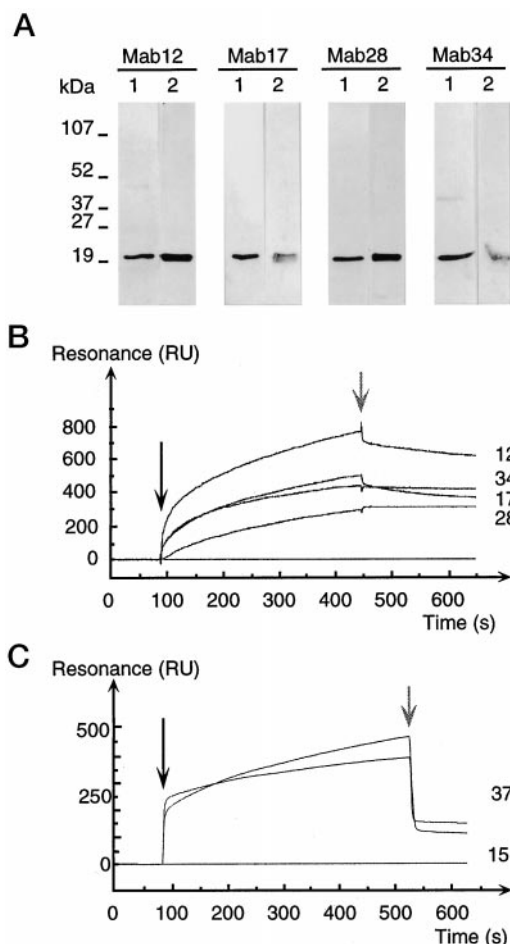
FIG. 1. **Interaction of mAbs to Nt-abp1 with partially purified** *E. coli* **Nt-abp1 and with Zm-abp1 purified from maize coleoptiles.** *A,* immunodetection of recombinant Nt-abp1 produced in *E. coli* and Zm-abp1 extracted from maize coleoptiles. After electrophoresis on SDS-acrylamide gel, proteins were transferred onto nitrocellulose membrane and probed with four IgG1 mAbs to Nt-abp1. *Lane 1* contains 50 ng of purified *E. coli* Nt-abp1 (*Ntt85* gene). *Lane 2* contains 250 ng of purified Zm-abp1. Molecular mass markers are indicated on the *left* in kDa. The overlay plot of four sensorgrams (*B*) illustrates the binding of IgG1-mAbs 12, 17, 28, and 34 to immobilized Nt-abp1. The interactions of IgM-mAbs 15 and 37 to immobilized Nt-abp1 are shown in *C*. The baseline (0) corresponds to the signal of continuous flow of HBS buffer over the matrix after immobilization of biotinylated Nt-abp1 on the sensor chip. The *black arrows* indicate the beginning of the injection of each mAb at about 0.3 μM over the matrix (association phase), and the *gray arrows* correspond to the end of the injection followed by a washing step in HBS buffer (dissociation phase).

abp1. The interactions between Nt-abp1 and mAbs have been studied using surface plasmon resonance. This method enables real-time measurements of the biospecific interactions, as shown in the resulting sensorgrams (Fig. 1, *B* and *C*). mAbs 12, 17, 28, and 34 bound rapidly to the immobilized Nt-abp1 protein, as shown by the slope of the curves (Fig. 1*B*) (31). The k_{off} values calculated from dissociation phases ranged from 3×10^{-5} to 10^{-5} M evincing a stable interaction of each mAb with Nt-abp1. No significant change of the interaction was observed when assayed at pH 5.7; conditions were similar to the electrophysiological experiments.

Interference Map—Surface plasmon resonance was used to monitor the binding of two distinct mAbs to establish the interference map of the different monoclonal antibody epitopes on Nt-abp1. The binding matrix shown in Fig. 2*A* results from interference experiments such as the one illustrated in Fig. 2*B*, which shows an overlay plot of two sensorgrams on immobilized Nt-abp1. The three consecutive injections of the first mAb,
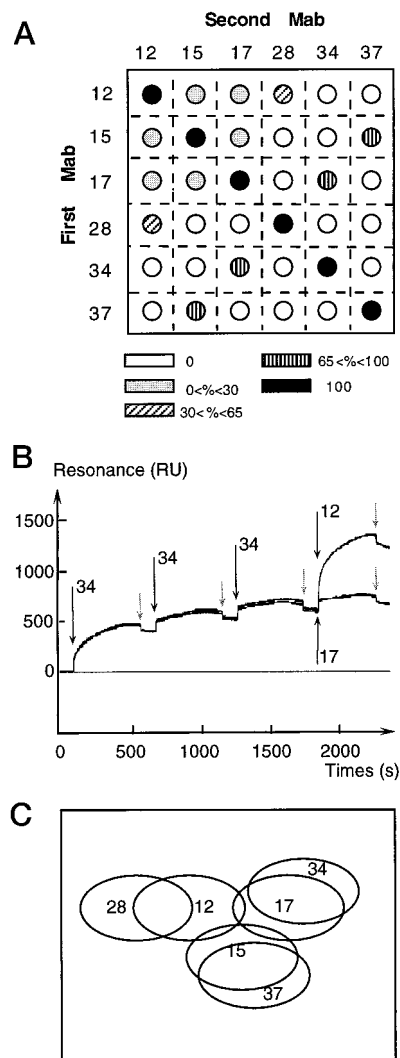

FIG. 2. **Binding pattern of the different mAbs to Nt-abp1 identified by pairwise epitope mapping using the biosensor.** *A,* binding matrix summarizing the results of pairwise epitope experiments. The reactivity of mAbs to similar epitopes of Nt-abp1 was tested by studying the ability of two mAbs to bind simultaneously to Nt-abp1. Noninteracting mAbs show 0% binding inhibition of the second mAb in the presence of the first one (*white circles*). *Shaded circles* illustrate a distinct percentage of inhibition reflecting weak to strong competition between mAb pairs as indicated by the key. *B,* overlay plot of two sensorgrams illustrating the sequence of injections performed to construct the binding matrix and the resulting interference map. Three consecutive injections of mAb 34 (first mAb) allow a saturation of the corresponding epitope. They are followed by the injection of either mAb 12 or mAb 17 (second mAbs). *C,* interference map illustrating the relative distribution of the different epitopes recognized by the mAbs on Nt-abp1. Each *oval* corresponds to the surface of interaction of a mAb with the protein (approximately 10 nm², radius of about 1.8 nm). *Nonoverlapping ovals* represent independent surfaces of interaction, and therefore included epitopes where the distance between the surface of interaction centers is at least of 3.6 nm (approximately 6–8 juxtaposed (not necessarily contiguous) residues) (38, 39). *Overlapping ovals* identify epitopes that cannot be totally reached at the same time by the corresponding mAbs; in this case the distance between the center of both surface is lower than 3.6 nm.

here mAb 34, allowed a saturation of the corresponding epitope. The capture of mAb 12 to the protein was not affected by prior binding of mAb 34, indicating that mAb 12 and mAb 34 do not interfere and recognize distant epitopes, whereas the capture of mAb 17 was reduced by about 80%. The interference between mAb 34 and mAb 17 demonstrates that their surfaces of interaction with the protein are overlapping. The interference map shown in Fig. 2*C* results from these analyses. Each
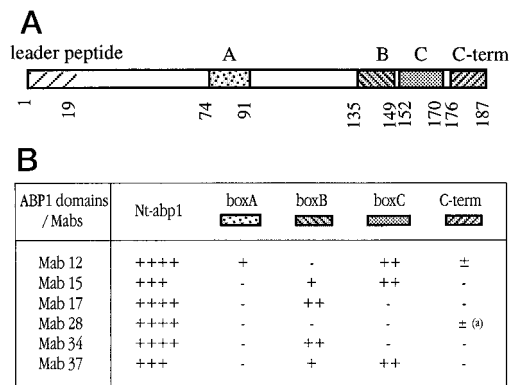
A

leader peptide   A   B C C-term

B

ABP1 domains / Mabs	Nt-abp1	boxA	boxB	boxC	C-term
Mab 12	++++	+	-	++	±
Mab 15	+++	-	+	++	-
Mab 17	++++	-	++	-	-
Mab 28	++++	-	-	-	± (a)
Mab 34	++++	-	++	-	-
Mab 37	+++	-	+	++	-

FIG. 3. **Interactions of mAbs with subdomains of Nt-abp1.** *A,* visualization of the synthetic peptides on the schematic linear representation of Nt-abp1. *Numbers* indicate the position of the amino acids for each peptide. *B,* the table summarizes results of direct and competitive binding experiments of mAbs to Nt-abp1 or synthetic peptides corresponding to particular domains of the protein. Interaction efficiencies are represented using a conventional scale from - to ++++ (on the basis of mole/mole interaction of the partners) to give a more comprehensive picture of the mAb interaction with Nt-abp1 and peptides. *(a)*, interaction observed only in competitive binding assays.

A

B

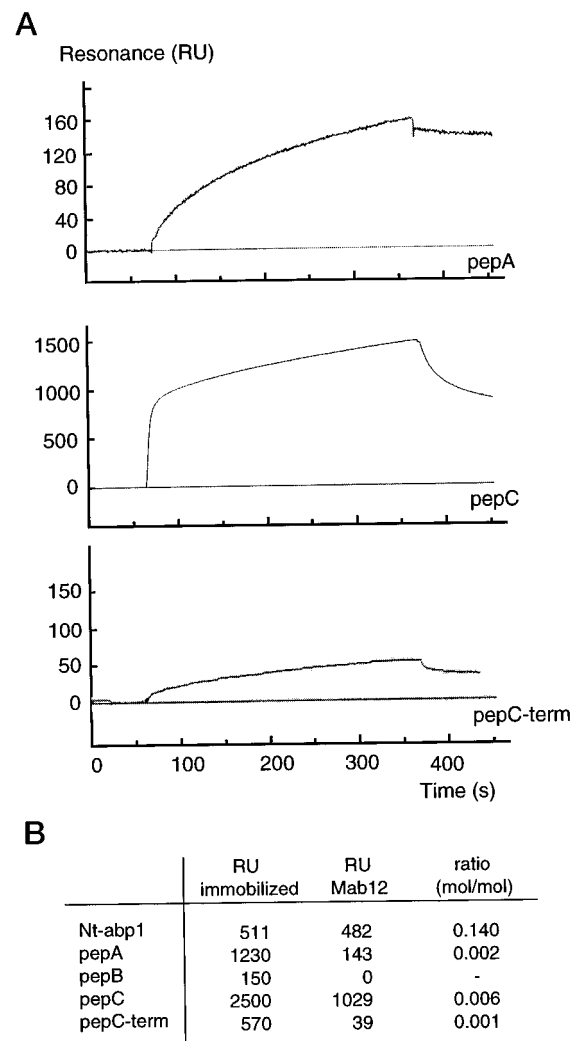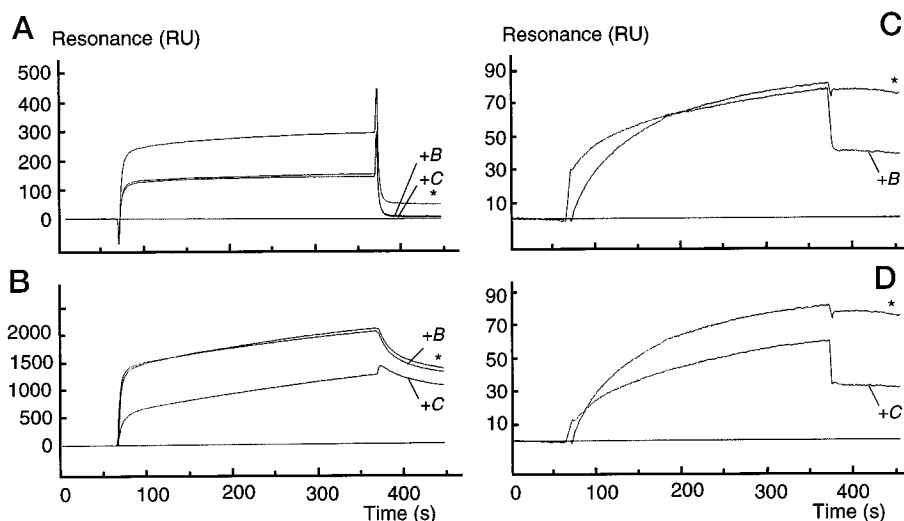|	RU immobilized	RU Mab12	ratio (mol/mol)
Nt-abp1	511	482	0.140
pepA	1230	143	0.002
pepB	150	0	-
pepC	2500	1029	0.006
pepC-term	570	39	0.001

FIG. 4. Interaction of mAb 12 with three synthetic peptides corresponding to box A, box C, and the C-terminal domain (*A*) of Nt-abp1 covalently linked to CM-dextran through amino groups. Resonance signals (*R*U) were plotted as a function of time. The association phases were followed through 300 s, after which the injection of mAb 12 was stopped and the dissociation phase in continuous buffer flow was monitored for 100 s. *B,* relative efficiencies of mAb 12 binding to the protein and the different peptides. Crude RU numbers of immobilized Nt-abp1 or synthetic peptide and captured mAb 12 are given. The ratio corresponds to the mole number of bound immunoglobulin mAb 12/mole number of covalently immobilized peptide on each sensorchip. Molecular mass used for the calculation were: IgG1 mAb 12 (150,000 Da), Nt-abp1 (22,000 Da), pep A and pep C (2400 Da), pep B and pepC-ter (2000 Da).

oval schematizes the surface of interaction of one mAb to the protein Nt-abp1. Taken together, the surfaces of interaction are distinct but form a large cluster. Inside of this cluster, the surfaces of interaction defined for mAb 17 and mAb 34 are closely overlapping, as also for mAb 15 and mAb 37, whereas the surfaces of interaction recognized by mAb 28, mAb 34, and mAb 37, and consequently their corresponding epitopes, are totally independent from one another. Within the cluster, mAb 12 fills a central position as it partially overlaps with the other three groups of independent mAbs.

Interaction Analysis of the mAbs with Nt-abp1 Domains— Further characterization of interactions of the different mAbs with Nt-abp1 was performed using a series of synthetic peptides covering part of the Nt-abp1 sequence (Fig. 3*A*). BIAcore technology was used for this analysis either by checking the direct recognition of the mAbs to the individual synthetic peptides immobilized on a sensor chip or by investigating the effect of these peptides on the interaction of the mAbs to the whole protein. The two distinct procedures are illustrated in Figs. 4 and 5 for mAb 12 and mAb 37, respectively. The sensorgrams shown in Fig. 4*A* illustrate the direct capture of mAb 12 on the immobilized peptides A, C, or C-term. mAb 12 associated slowly with the peptide A and even more slowly with the C-term peptide but in both cases the association was stable as no dissociation was observed after washing. Binding of mAb 12 to pep C was extremely rapid but was counteracted by dissociation as the interaction was unstable. To evaluate the relative efficiency of interaction between mAb 12, the protein, and the different peptides, we compared the number of mAb 12 RU bound in 6 min of injection to each captor taking into account the amount of protein or peptide immobilized on the matrix and the molecular weight of the interacting molecules (Fig. 4*B*). The ratio of mAb 12 IgG bound to immobilized protein or peptide, expressed in mole/mole, is 25–150-fold higher with the whole protein than with each interacting synthetic peptide.

Competitive binding assays of mAbs in the presence of an excess of synthetic peptide are illustrated for mAb 37 (Fig. 5). The addition of peptides B or C to mAb 37 produced a strong reduction of mAb 37 capture on the immobilized Nt-abp1 (Fig. 5*A*), indicating that both interact specifically with the site of recognition. Both peptides decreased the score of mAb 37 binding to the immobilized peptide B (Fig. 5, *C* and *D*), whereas peptide B competed poorly with the interaction between mAb

37 and the immobilized peptide C (Fig. 5*B*). Direct binding of mAb 37 (not shown) proved that its interaction with peptide C is stronger than with peptide B, which explains the differences observed in the competitive binding assays. The two peptides therefore interact specifically with mAb 37 and constitute part of the corresponding epitope. Similar results were obtained with mAb 15 (data not shown) thus confirming the proximity of mAb 15 and mAb 37 epitopes as indicated in Fig. 2, *A* and *C*.

Fig. 3*B* summarizes the results of the direct and competitive assays. All the mAbs exhibited a stronger interaction with the whole protein than with the individual synthetic peptides. Different mAbs bound independently one or a number of synthetic peptides (as shown for mAb 12 or 37 in Figs. 4 and 5, respectively) with the exception of mAb 28 for which no direct binding was detected. However, a slight effect of the C-terminal peptide was observed in competitive binding of mAb 28 on Nt-abp1.

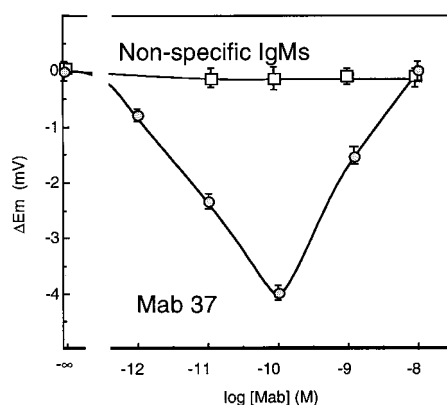FIG. 7. **Effects of mAb 37 on the transmembrane potential of tobacco mesophyll protoplasts.** Tobacco mesophyll protoplasts were incubated for 5 min at room temperature in the presence of mAb 37 (○), or nonspecific antibodies (□). Measurements of E_m values of 15 individual protoplasts were performed in each condition. In dose-response curves, E_m variations (ΔE_m) obtained in one representative experiment of three are plotted as a function of antibody concentrations in the external medium. Standard errors did not exceed 0.4 mV

enough to be detected when one domain is out of the Nt-abp1 context.

Nt-abp1 Folding—The study of the interaction of the mAbs to Nt-abp1 and the different peptides has provided a unique insight into the folding of the protein. The detailed study of mAb 12 indicates that the A and C boxes and the C terminus of the protein are assembled when the protein is folded. It is of particular significance that the A and C boxes of Nt-abp1 are brought together in a conformational state of the protein. From early studies, a number of amino acid residues (Cys, His, Tyr/Lys, Asp/Glu, and Arg) were provisionally identified to be present at the auxin active site of an interacting protein (33, 34). Five of these residues were found within box A of ABP1, and a polyclonal antibody (23) to a synthetic peptide comprising these residues was shown to mimic the auxin effect on the electrophysiological assay of tobacco protoplasts. These arguments have designated box A as a good candidate to form the auxin binding site of ABP1. Using photoaffinity labeling reagent (tritiated 5-azidoindole-3-acetic acid) and microsequence analysis of photolabeled ABP1 tryptic fragments, Brown and Jones (24) have shown that a unique peptide, corresponding to the box C, was labeled suggesting the involvement of Asp, His, or Trp residues contained in this box. The authors hypothesized that the auxin binding site of ABP1 could be formed by residues located in both box A and box C. Specifically, the hydrophobic platform could be formed by Trp[158] (from box C, amino acid number corresponding to Nt-abp1 sequence), and the carboxylic acid binding site could be formed by the positive charge of the cluster His-Arg[79]-His (from box A). Our results support this hypothesis by showing that box A and box C are closely related in the folded protein and can both participate in the binding of auxin.

In addition, our results show that the C terminus is also associated with the A and C boxes. The box A and the C terminus both contain a cysteine residue that are thus brought together; the third cysteine residue being located at the N terminus. We propose that, in the conformational state studied here, the protein could be stabilized by a disulfide bridge formed between Cys[82] (box A) and Cys[177] (C-terminal peptide). Using the ELISA procedure, Napier and Venis (35) have reported that millimolar NAA blocked the binding of an antibody (MAC 256) to the C terminus of the maize ABP1, suggesting that this domain is modified or partly concealed after auxin binding. However, the concentration of auxin needed to induce

such a change was relatively high, making it difficult to draw conclusions on the physiological significance of this observation. Auxin binding has also been demonstrated to be reversibly inactivated by reducing agents, suggesting the presence of a reducible group, possibly a disulfide, located at the auxin binding site and essential for binding activity (33, 36). The proximity between the C-terminal domain (including the Cys[177]) and the two boxes involved in auxin binding provides a new interpretation of earlier data. One explanation is that polar and charged residues of the C-terminal domain are also directly involved in the binding of auxin, although this has not been revealed using labeled azido-auxin (24). Alternatively, this domain may contribute indirectly to the interaction with auxin by its role in the folding of ABP1 through disulfide bridge formation between Cys[177] and Cys[82].

Nt-abp1 Is Acting at the Plasma Membrane—Following its isolation, the maize ABP1 was quickly designated as a putative auxin receptor. However, experimental evidence supporting this hypothesis has been based largely on functional assays performed using a restricted number of heterologous tools on tobacco cells. To assess the possible involvement of Nt-abp1 in an early step of auxin action, the whole panel of mAbs to Nt-abp1 has been used in the auxin electrophysiological assay on tobacco protoplasts providing for the first time homologous conditions. All the antibodies were shown to modify the electrical response of tobacco protoplasts demonstrating three important features. First, the protein involved in auxin signaling at the outer face of the plasma membrane is recognized by the nine distinct mAbs. Second, the interacting protein at the plasma membrane and Nt-abp1 share the 9 distinct epitopes indicating that the antigenic pattern is identical and that Nt-abp1 itself is present at the surface of the plasma membrane and is involved in the activation of the auxin electrical response. Third, we have shown that most of the mAbs interact with discontinuous epitopes using recombinantly expressed protein. The results suggest that the conformation-dependent epitopes are present on the native protein at the surface of tobacco protoplasts.

Modulation of Nt-abp1 Activity in Auxin Signaling Using Specific mAbs—Two kinds of effects have been observed in the presence of the anti-Nt-abp1 mAbs on the electrical response of tobacco protoplasts. Several mAbs such as mAb 12, 17, or 34 inhibit the auxin-induced response, suggesting that they blocked the transduction cascade involving ion fluxes responsible for the hyperpolarization. As we have demonstrated above, mAb 12 spans three distinct domains of the protein overlapping the auxin binding site and very efficiently blocking auxin action. The mAbs showing antagonist activity on the electrical response could block auxin binding either by sterically occupying at least part of the auxin binding domain, immobilizing the protein in a particular conformation, or by inducing a conformational change incompatible with the activation of the transduction cascade.

Another kind of effect was observed with two totally distinct mAbs, mAb 37 and mAb 28, which were shown to interact with nonoverlapping epitopes (Fig. 2). These mAbs mimic auxin action on the electrical response in the absence of the hormone in the medium (Fig. 7). Such hormonomimetic action has previously been reported for a polyclonal antibody, named D16, raised against a synthetic peptide corresponding to the box A of the maize ABP1 (23). It was originally interpreted as a strong indication that D16 IgGs were acting at the ligand binding site of ABP1 (23), acting similarly as an anti-idiotypic antibody. Our results demonstrated that such a hormonomimetic effect can arise from interaction of mAbs with distinct domains. We propose that the common feature is the conformational change

of Nt-abp1 evoked by the immunoglobulin binding. The site of the antibody interaction can be superposed with the auxin binding site or can be distinct from it. Interestingly, the epitopes of mAb 12 and mAb 28 overlap, whereas they provoke opposite effects on the electrical response. The region formed by the assembly of boxes A and C and the C-terminal domain appears to be a critical region for Nt-abp1 versatile enough to act as a switch for active conformational change of the protein. Auxin-induced conformational change has been reported in Zm-abp1 from circular dichroism spectroscopy measurements (37) and ELISA experiments (35). For the activation of the auxin electrical response, the most important step appears to be the induction of the conformational change of Nt-abp1 resulting in a modification of its interaction with the plasma membrane.

In conclusion, we confirmed unambiguously that Nt-abp1 is present at the plasma membrane and is involved in the activation of at least one auxin-dependent response, namely an early and specific electrical response to auxin at the plasma membrane. The conformation adopted by Nt-abp1 after interaction with auxin or specific antibodies leads to the activation or inhibition of the auxin signal transduction cascade. The challenge now will be to further understand the mechanisms of interaction between Nt-abp1 and the plasma membrane as well as correlating the early electrical response induced by auxin to later auxin events at the molecular and cellular levels. A preliminary indication has recently been provided by Jones *et al.* (19), showing that ABP1-overexpressing plants exhibit an increased capacity for auxin-mediated cell expansion. The panel of mAbs that we have obtained to Nt-abp1 provides a unique set of molecular tools to follow up the functional study of Nt-abp1 and its role in the control of physiological auxin responses.

REFERENCES

1. Davies, P. J. (1995) in *Plant Hormones: Physiology, Biochemistry and Molecular Biology* (Davies, P. J., ed) pp. 1–38, Kluwer Academic Publishers, The Netherlands
2. Abel, S., and Theologis, A. (1996) *Plant Physiol.* (*Bethesda*) **111,** 9–17
3. Guilfoyle, T., Hagen, G., Ulmasov, T., and Murfett, J. (1998) *Plant Physiol.* (*Bethesda*) **118,** 341–347
4. Del Pozo, J. C., Timpte, C., Tan, S., Callis, J., and Estelle, M. (1998) *Science* **280,** 1760–1763
5. Walker, L., and Estelle, M. (1998) *Curr. Opin. Plant Biol.* **1,** 434–439
6. Venis, M. A., and Napier, R. M. (1995) *CRC Crit. Rev. Plant Sci.* **14,** 27–47
7. Jones, A. M. (1994) *Annual Review of Plant Physiology and Plant Molecular Biology* (Jones, R. L., Somerville, C. R., and Walbot, V., eds) Vol. 45, pp. 393–420, Annual Reviews, Inc., Palo Alto, CA
8. Löbler, M., and Klämbt, D. (1985) *J. Biol. Chem.* **260,** 9848–9853
9. Tillmann, U., Viola, G., Kayser, B., Siemeister, G., Hesse, T., Palme, K., Löbler, M., and Klämbt, D. (1989) *EMBO J.* **8,** 2463–2467
10. Barbier-Brygoo, H., Ephritikhine, G., Klämbt, D., Ghislain, M., and Guern, J. (1989) *Proc. Natl. Acad. Sci. U. S. A.* **86,** 891–895
11. Barbier-Brygoo, H., Ephritikhine, G., Klämbt, D., Maurel, C., Palme, K., Schell, J., and Guern, J. (1991) *Plant J.* **1,** 83–93
12. Rück, A., Palme, K., Venis, M. A., Napier, R. M., and Felle, R. H. (1993) *Plant J.* **4,** 41–46
13. Zimmermann, S., Thomine, S., Guern, J., and Barbier-Brygoo, H. (1994) *Plant J.* **6,** 707–716
14. Thiel, G., Blatt, M. R., Fricker, M. D., White, I. R., and Millner, P. (1993) *Proc. Natl. Acad. Sci. U. S. A.* **90,** 11493–11497
15. Venis, M. A., Thomas, E. W., Barbier-Brygoo, H., Ephritikhine, G., and Guern, J. (1990) *Planta* **1,** 232–235
16. Barbier-Brygoo, H., Zimmermann, S., Thomine, S., White, I. R., Millner, P., and Guern, J. (1996) *Plant Growth Regul.* **18,** 23–28
17. Napier, R., and Venis, M. A. (1992) *Biochem. J.* **284,** 841–845
18. Hertel, R. (1995) *J. Exp. Bot.* **46,** 461–462
19. Jones, A. M., Im, K. H., Savka, M. A., Wu, M. J., DeWitt, N. G., Shillito, R., and Binns, A. N. (1998) *Science* **282,** 1114–1117
20. Leblanc, N., Perrot-Rechenmann, C., and Barbier-Brygoo, H. (1999) *FEBS Lett.* **449,** 57–60
21. Leblanc, N., Roux, C., Pradier J. M., and Perrot-Rechenmann, C. (1997) *Plant Mol. Biol.* **33,** 679–689
22. Napier, R. M., Venis, M. A., Bolton, M. A., Richardson, L. I., and Butcher, G. W. (1988) *Planta* **176,** 519–526
23. Venis, M. A., Napier, R. M., Barbier-Brygoo, H., Maurel, C., Perrot-Rechenmann, C., and Guern, J. (1992) *Proc. Natl. Acad. Sci. U. S. A.* **89,** 7208–7212
24. Brown, J. C., and Jones, A. M. (1994) *J. Biol. Chem.* **269,** 21136–21140
25. Nowinski, R. C., Lonstrom, M. E., Tam, M. R., and Burnette, W. R. (1979) *Virology* **93,** 111–126
26. Johnsson, B., Löfas, S., and Lindquist, G. (1991) *Anal. Biochem.* **198,** 268–277
27. Panayotou, G., Waterfield, M. D., and End, P. (1993) *Curr. Biol.* **3,** 913–915
28. Lacey, E., and Grant, W. N. (1987) *Anal. Biochem.* **163,** 151–158
29. Caboche, M. (1980) *Planta* **149,** 7–18
30. Ephritikhine, G., Barbier-Brygoo, H., Muller, J. F., and Guern, J. (1987) *Plant Physiol.* (*Bethesda*) **83,** 801–804
31. Karlsson, R., Roos, H., Fägerstam, L., and Persson, B. (1994) *Methods: A Companion to Methods in Enzymology* (Abelson, J. N., and Simon, M. I., eds) Vol. 6, pp. 99–110, Academic Press, Orlando, FL
32. Dubs, M. C., Altschuh, D., and Van Regenmortel, M. H. V. (1992) *J. Chromatogr.* **597,** 391–396
33. Venis, M. A. (1977) *Planta* **134,** 145–149
34. Navé, J. F., and Benveniste, P. (1984) *Plant Physiol.* (*Bethesda*) **74,** 1035–1040
35. Napier, R. M., and Venis, M. A. (1990) *Planta* **182,** 313–318
36. Ray, P. M., Dohrmann, U., and Hertel, R. (1977) *Plant Physiol.* (*Bethesda*) **59,** 357–364
37. Shimomura, S., Sotobayashi, T., Futai, M., and Fukui, T. (1986) *J. Biochem.* **99,** 1513–1524
38. Cunningham, B. C., and Wells, J. A. (1989) *Science* **244,** 1081–1085
39. Poljak, R. J., Anzel, L. M., Chen, B. L., Phizackerley, R. P., and Saul, F. (1974) *Proc. Natl. Acad. Sci. U. S. A.* **71,** 3440–3444